Combination of chiroptical, absorption and fluorescence spectroscopic methods reveals multiple, hydrophobicity-driven human serum albumin binding of the antimalarial atovaquone and related hydroxynaphthoquinone compounds

Ferenc Zsila* and Ilona Fitos

Received 13th May 2010, Accepted 21st July 2010
DOI: 10.1039/c0ob00124d

High-affinity human serum albumin (HSA) binding of the C3-substituted antimalarial 2-hydroxy-1,4-naphthoquinone derivative atovaquone (ATQ) has been demonstrated and studied by circular dichroism (CD), UV/VIS absorption, fluorescence spectroscopy and affinity chromatography methods. The analysis of induced CD data generated upon HSA binding of ATQ revealed two high-affinity binding sites ($K_a \approx 2 \times 10^6$ M^{-1}). CD interaction studies and displacement of specific fluorescent and radioactive marker ligands indicated the contribution of both principal drug binding sites of HSA to complexation of ATQ, and also suggested the possibility of simultaneous binding of ATQ and some other drugs (*e.g.* warfarin, phenylbutazone, diazepam). Comparison of UV/VIS spectra of ATQ measured in aqueous solutions indicated the prevalence of the anionic species formed by dissociation of the 2-hydroxyl group. HSA binding of related natural hydroxynaphthoquinones, lapachol and lawsone also induces similar CD spectra. The much weaker binding affinity of lawsone ($K_a \approx 10^4$ M^{-1}) bearing no C3 substituent highlights the importance of hydrophobic interactions in the strong HSA binding of ATQ and lapachol. Since neither drug exhibited significant binding to serum α_1-acid glycoprotein, HSA must be the principal plasma protein for the binding and transportation of 2-hydroxy-1,4-naphthoquinone-type compounds which are ionized at physiological pH values.

Introduction

Atovaquone (ATQ), a substituted hydroxynaphthoquinone derivative, is a broad spectrum anti-infective drug, showing activity against various *Plasmodium* species and other protozoa including *Pneumocystis carinii* and *Toxoplasma gondii*.[1,2] ATQ is structurally related to ubiquinone and competitively inhibits its binding to the cytochrome bc_1 complex of the parasite mitochondrial electron transport chain, thereby inhibiting several metabolic enzymes. Very high plasma protein binding (99.9%) and metabolic stability of ATQ have been reported and thought to contribute to its long plasma half-life (70 h) in humans.[3,4] The dependence of the ATQ-mediated *in vitro* inhibition of cytochrome P_{450} (CYP)2C9 on the plasma protein content of the medium used has also been noted.[5] Since no details are available on the plasma protein binding of ATQ, the present work is aimed to investigate binding interactions of ATQ with the main drug carrier components of blood, human serum albumin (HSA) and α_1-acid glycoprotein (AAG). Previously, AAG binding of several basic antimalarial drugs has been successfully studied by using circular dichroism (CD) and UV/VIS absorption spectroscopy techniques.[6] The naphthoquinone chromophore of ATQ having several electronic transitions above 250 nm allowed the application of these methodologies for verifying and analysing HSA binding of ATQ and two related natural compounds—lawsone (LWS) and lapachol (LPC) (Fig. 1).

Department of Molecular Pharmacology, Institute of Biomolecular Chemistry, Chemical Research Center, H-1025 Budapest, Pusztaszeri út 59-67, Hungary. E-mail: zsferi@chemres.hu; Fax: (+36) 1-438-1145

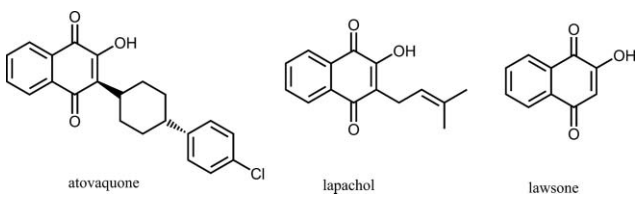

Fig. 1 Chemical structures of atovaquone (*trans*-2-hydroxy-3-(4-chlorophenyl-cyclohexyl)-1,4-naphthoquinone), lapachol (2-hydroxy-3-(3′-methyl-2-butenyl)-1,4-naphthoquinone) and lawsone (2-hydroxy-1,4-naphthoquinone).

Materials and methods

Materials

Atovaquone (98.9%) was a gift from GlaxoSmithKline (Greenford, Middlesex, United Kingdom). Lawsone (Sigma), lapachol (Aldrich), indomethacin (Fluka), (±)-flurbiprofen (Sigma), dansyl-L-asparagine (Sigma), dansylsarcosine (Sigma), 5-dimethylaminonaphthalene-1-sulfonamide, phenylbutazone (Sigma), diazepam (Sigma), and (±)-warfarin (Sigma) were used as supplied. HSA (97%, essentially fatty acid-free) and AAG (99%, purified from Cohn Fraction VI) were purchased from Sigma and used without further purification. [^{14}C]Diazepam and [^{14}C](±)-warfarin (both 56 mCi $mmol^{-1}$) were obtained from Amersham, GE Healthcare UK, and were used for labelling inactive ligand solutions. HPLC grade ethanol and diluted NaOH (flurbiprofen, warfarin) were used to prepare ligand stock solutions.

Preparation of HSA and AAG sample solutions

Protein samples were dissolved in physiological Ringer buffer solution (pH 7.4; 137 mM NaCl, 2.7 mM KCl, 0.8 mM $CaCl_2$, 1.1 mM $MgCl_2$, 1.5 mM KH_2PO_4, 8.1 mM $Na_2HPO_4 \cdot 12H_2O$, and 1.5 mM NaN_3). Concentration of HSA and AAG were determined by weight (M_w of 66400 and 40000).

Circular dichroism and UV/VIS absorption spectroscopy measurements

CD and UV/VIS spectra were recorded on a Jasco J-715 spectropolarimeter at 37 ± 0.2 °C. Temperature control was provided by a Peltier thermostat equipped with magnetic stirring. For recording CD spectra, rectangular quartz cells of 1 cm optical path length (Hellma, USA) were used. Each spectrum represents the average of three scans obtained by collecting data at a scan speed of 100 nm min^{-1}. UV/VIS absorption spectra were obtained by conversion of the high voltage (HT) values of the photomultiplier tube of the CD equipment into absorbance units. CD and absorption curves of drug–protein mixtures were corrected by subtracting the spectra of protein solutions.

JASCO CD spectropolarimeters record CD data as ellipticity ('Θ') in units of millidegrees (mdeg). The quantity of 'Θ' is converted to '$\Delta\varepsilon$' values using the equation $\Delta\varepsilon = \Theta/(32982cl)$, where '$\Delta\varepsilon$' is the molar circular dichroic absorption coefficient expressed in M^{-1} cm^{-1}, 'c' is the molar concentration of the ligand (mol L^{-1}), and 'l' is the optical path length expressed in cm.

Calculation of HSA binding parameters of ATQ, LPC and LWS from CD data

Details of the estimation of the association constants (K_a) and the number of binding sites (n) using CD spectroscopic data have been described previously.[7] Non-linear regression analysis of the CD values measured at different [drug]/[HSA] molar ratios was performed by the NLREG® software (statistical analysis program, version 3.4 created by Philip H. Sherrod).

Fluorescence measurements

Fluorescence measurements were carried out in a Shimadzu RF-1501 spectrofluorophotometer at room temperature (24 ± 1 °C), using quartz cuvette with 1 cm optical path length, both bandwidths were 10 nm. Aliquots of 2 mL HSA solutions were measured alone, as well as in the presence of labels and displacers. Fluorescence intensities were corrected for the inner filter effects according to the absorbance of the additive at both the excitation and emission wavelengths,[8] as well as for the quenching due to ethanol content of additive stock solutions. Fluorescence of free labels and additives was negligible. The quenching effects were characterized[8] with the quenching constants (K_{sv}) according to the Stern–Volmer equation ($F_0/F = 1 + K_{sv}$[quencher]).

Ultrafitration

Ultrafiltration was performed at room temperature in an Amicon MPS-1 system by centrifugation using YMT 30 membrane discs (Millipore). Free fractions of the radioactively labelled ligands were measured in duplicate by liquid scintillation counting. Protein–ligand solutions contained 1% ethanol. Non-specific binding of radioactive markers was negligible.

Affinity chromatography

Chromatographic experiments on HSA–Sepharose gel were performed as described previously.[9] HSA (fatty acid free, Sigma) in 1% concentration was immobilized on CNBr-activated Sepharose 4B (Pharmacia) and the gel was filled into a glass column. Elution was made by Ringer buffer at room temperature, the flow rate was 1 mL min^{-1}. Ligand samples (5–20 µl of 2 mM ethanolic stock solutions) were applied and elution volumes were determined by UV detection. Control experiments performed on a gel containing no HSA showed no retentions.

Results

CD and UV/VIS spectroscopic investigation of HSA binding of ATQ

Acidified ethanolic solution of ATQ exhibits yellow colour due to the medium intensity absorption band around 390 nm, the tail of which does not extend over 460 nm (Fig. 2). Upon addition of the ethanolic solution of ATQ into the Ringer buffer solution of HSA, however, the mixture promptly turns pink due to the appearance of a new, broad VIS absorption band between 400–600 nm. Absorbance of this peak increased gradually by raising the [ATQ]/[HSA] ratio of the sample, without alteration of its shape or position (not shown). In HSA solution, the 334 and 387 nm peaks of ATQ recorded in EtOH cannot be seen as separate bands (Fig. 2), the UV peak observed at 253 nm in EtOH is completely absent, while the band at 278–283 nm (EtOH) gains intensity and exhibits significant broadening with two shoulders, on the short- and long-wavelength sides. However, all of these UV/VIS spectral alterations can be reconstructed in the absence of HSA

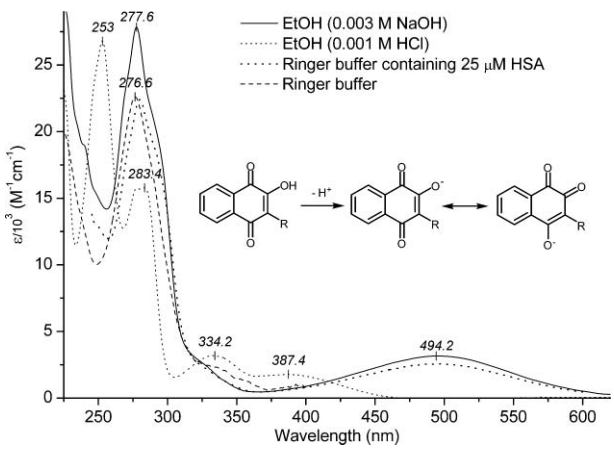

Fig. 2 UV/VIS absorption spectra of ATQ measured in EtOH under acidic and alkaline conditions (20 °C) and in pH 7.4 Ringer buffer solution in the absence and in the presence of equimolar HSA (37 °C, [ATQ]/[HSA] = 1). In protein-free Ringer solution ([ATQ] = 4 µM) the absorption curve ends at 400 nm since no reliable absorbance data could be measured above this wavelength. EtOH content of the buffer solutions was ≤2 v/v%. Inset shows the dissociation of the acidic 2-hydroxy group and mesomeric forms of the anionic species.

as well. The UV/VIS spectrum of ATQ in alkaline EtOH is very similar to that measured in HSA solution (Fig. 2). Though the water solubility of the strongly lipophilic ATQ (log $P_{octanol/water}$ of 5.31) is very limited (0.43 μg ml^{-1} ≈ 1 μM),[10] the intensity of the π–π*-type UV band below 300 nm is high enough to obtain a reliable absorption curve even at low concentration. The UV spectrum of 1.5 μg ml^{-1} ATQ in Ringer buffer at 37 °C is similar to that obtained in HSA solution (Fig. 2). In relation to the λ_{max} values measured in protein-free aqueous environment, HSA binding caused a red shift of the UV/VIS absorption peaks of ATQ (Fig. 3).

CD experiments showed that absorption bands of ATQ recorded in HSA solution were associated by multiple induced Cotton effects (CEs) both in the UV and in the VIS region of the CD spectrum (Fig. 3). The most intense induced CD (ICD) band is shown at 275 nm, the λ_{max} of which is blue-shifted by 5 nm in comparison to the UV absorption peak. Above 300 nm the CD intensities are weaker by an order of magnitude, thus the spectra were taken at higher HSA and ATQ concentrations. The broad, low-intensity negative ICD peak around 522 nm is allied to the VIS absorption band; no separate absorption band belongs, however, to the twice as intense negative CE at 406 nm. Upon raising the ATQ concentration in the HSA sample solution the ICD values increased without other spectral alterations (data not shown). Two sets of ICD data detected at 275 and 406 nm at increasing [ATQ]/[HSA] ratios were plotted to calculate the HSA association constant and number of binding sites (Fig. 4). The K_a and n values estimated from the ICD data measured at 275 and 406 nm are close to each other, suggesting multiple, high-affinity albumin binding of ATQ.

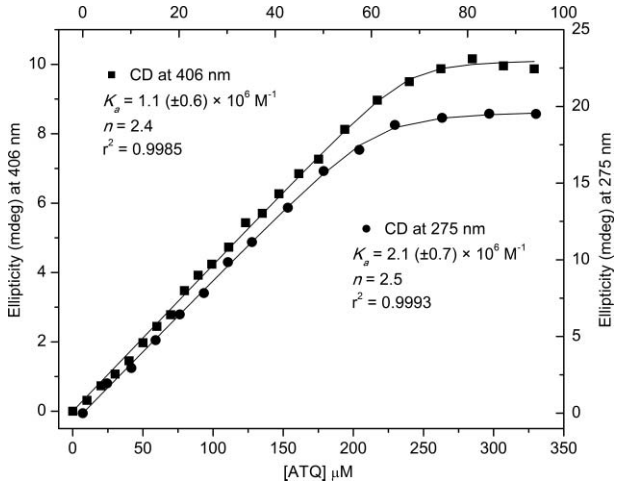

Fig. 4 Calculation of HSA binding parameters of ATQ from ICD data measured in a pH 7.4 Ringer buffer at 37 °C. CD values measured at 406 (bottom 'X', left 'Y', [HSA] = 100 μM) and 275 nm (top 'X', right 'Y', [HSA] = 25 μM) are plotted *vs.* molar concentrations of ATQ. *Squares and circles*: experimental CD data points. *Solid lines*: results of the curve fitting procedure. At the end of the titrations the EtOH content of the samples were 7 and 2 v/v%, respectively.

Characterization of HSA binding sites of ATQ by CD displacement experiments

In order to identify albumin binding sites of ATQ, CD displacement measurements were performed by using some drugs which are known to bind specifically to the principal drug binding sites of HSA called drug site I and II.[11] Since ICD activity in protein

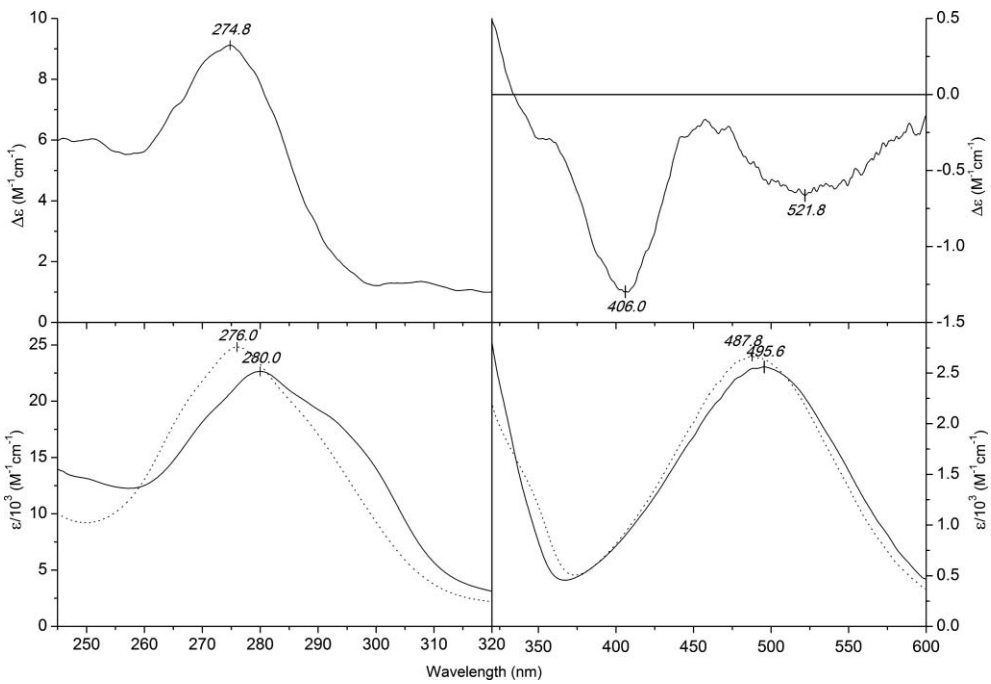

Fig. 3 Difference CD and UV/VIS absorption spectra of ATQ in HSA solution (solid line) and in alkaline water (dotted line) at 37 °C. Left panels: [ATQ] = [HSA] 25 μM. Right panels: [ATQ] = 110 μM, [HSA] = 100 μM. Molar CD (Δε) and absorption (ε) values were calculated on the basis of total drug concentration of the sample solutions.

solution reflects the bound drug concentration, it will vanish upon addition of a ligand having the same binding site. This approach can be successfully applied for mapping binding sites of guest compounds.[12] Indomethacin (IND), phenylbutazone (PHN), and (±)-warfarin (WRF) were used as the marker ligands of drug site I located in subdomain IIA.[11] In order to fully saturate both ATQ binding sites of HSA, [ATQ]/[HSA] = 2 ratio was set in sample solutions, which were titrated by small aliquots of concentrated stock solution of the additive. Long-wavelength negative CEs of ATQ were monitored which do not interfere with the own CEs of IND, PHN, and WRF induced below 360 nm.[13–15] Addition of IND affected both CEs in an opposite manner (Fig. 5): the intensity of the 406 nm ICD band decreased gradually upon elevation of IND concentration but no complete extinction of this band could be achieved even at a high excess of the displacer. In contrast, the magnitude of the 520 nm CE increased slightly in the presence of IND. Addition of PHN (Fig. 5) and WRF (not shown) resulted in even greater intensification of the CE at 520 nm, but distinct from IND, hardly affected the CE at 406 nm (Fig. 5). During displacement experiments the absorption curve of ATQ showed no change (not shown). (±)-Flurbiprofen (FLB), the high-affinity marker ligand of site II in subdomain IIIA, after a transient increase of the CE at 520 nm decreased the magnitudes of both CEs of ATQ (Fig. 6). The high-excess of FLB at the end of the titration rendered the sample opalescent presumably due to the aqueous aggregation of the displaced ATQ molecules. The UV CE of ATQ could not be investigated due to the ICD activity of HSA-bound FLB below 300 nm.[13] Diazepam (DZP) is also a

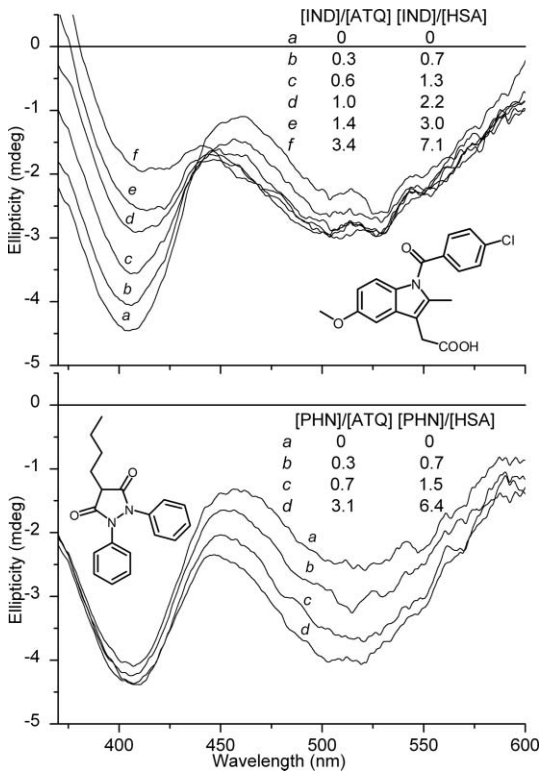

Fig. 5 Changes of difference CD spectra of ATQ upon increasing concentration of site I marker ligands IND (top) and PHN (bottom). [HSA] = 50 μM, [ATQ] = 100 μM. At the end of the titrations the EtOH content of both samples was 5 v/v%.

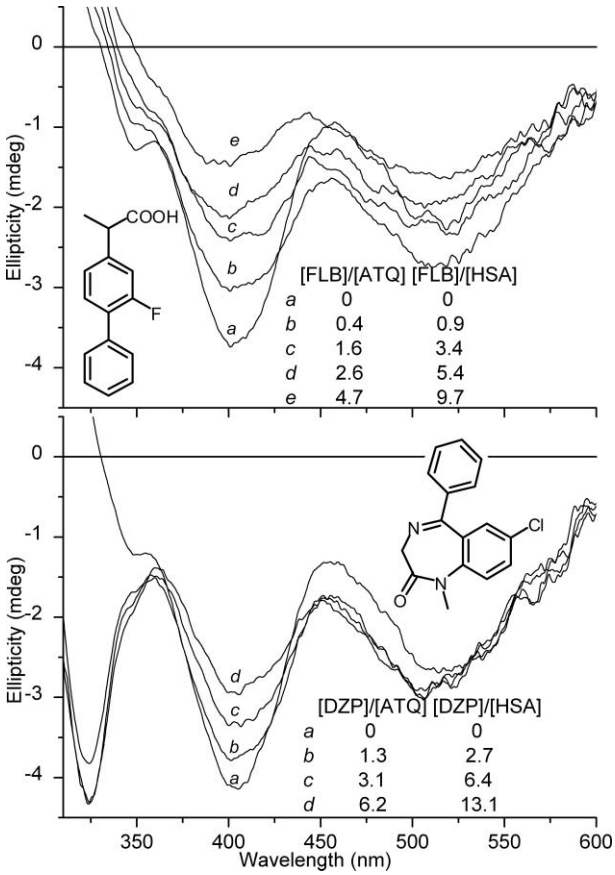

Fig. 6 Changes of difference CD spectra of ATQ upon increasing concentration of site II marker ligands FLB (top) and DZP (bottom). [HSA] = 50 μM, [ATQ] = 100 μM. At the end of the titrations the EtOH content of both samples was 6 v/v%.

marker drug of the site II of HSA.[11] Distinct from FLB, however, addition of DZP had no significant effect on the CE of ATQ at 520 nm and it caused only ≈30% intensity loss in the amplitude of the 406 nm ICD peak (Fig. 6). During the course of the titration with DZP, a novel negative CE developed at 324 nm showing no further intensity increase after reaching a [DZP]/[HSA] ratio of 4. This band belongs to DZP, attributed to the preferential HSA binding of the chiral *M*-conformer of the benzodiazepine ring.[16]

In summary, only FLB seems to be able to inhibit ATQ binding, but each investigated drug affected it.

Displacement of radioactive markers by ATQ

DZP and WRF are characteristic markers of the two main drug binding sites of HSA,[17] located in subdomains IIIA and IIA, respectively.[18] The effect of ATQ on the binding of radioactively labelled DZP and WRF can be seen in Table 1. The measured free fractions for DZP and WRF correspond to binding constants of 1.2×10^5 M^{-1} and 1.5×10^5 M^{-1}, respectively. The displacements measured in the presence of ATQ correspond to $3(\pm1) \times 10^4$ M^{-1} inhibition constants in both cases, assuming simple competition. This value is much lower compared to that determined for ATQ binding by the ICD method (Fig. 4). Thus, the observed displacements are probably due to non-competitive interactions. It means that the binding sites of ATQ are not identical to those

Table 1 Effect of ATQ on the binding of [^{14}C]DZP and [^{14}C](±)-WRF to HSA measured by ultrafiltration

	12 μM [^{14}C]DZP 15 μM HSA	12 μM [^{14}C] (±)-WRF 15 μM HSA
[ATQ] μM	free fraction of DZP	free fraction of (±)-WRF
—	0.48 (±0.02)	0.44 (±0.02)
10	0.55 (±0.02)	0.47 (±0.02)
20	0.57 (±0.02)	0.51 (±0.02)
40	0.64 (±0.03)	0.64 (±0.03)

of DZP and WRF. It is in accordance with the CD displacement results.

CD-UV/VIS spectroscopy of LPC–HSA complexes

LPC, originally isolated from species of the *Bignoniaceae* family, exhibits a wide range of therapeutic activities including antimalarial, trypanocidal, anticancer and anti-inflammatory properties.[19] Since the hydroxynaphthoquinone nucleus of LPC and ATQ is identical and the molecules differ only in the structure of the C3 substituent, UV/VIS spectroscopic profiles of LPC measured in acidic EtOH (yellow) and in HSA solution (pink) are very similar to those found with ATQ (Fig. 7). The binding of LPC to HSA also induced two negative CEs above 330 nm with shapes and λ_{max} values close to those recorded for ATQ–HSA complexes (Fig. 7). However, the intensity ratio of these peaks differs, in the case of LPC the longest-wavelength CE is more intense. In the UV region a dominant positive ICD peak was found at 275 nm, which is very similar to the analogous band measured with ATQ (*cf.* Fig. 3). However, a negative ICD band was also developed with a λ_{max} of 298 nm (Fig. 7). In the same region the ICD values of ATQ are positive, though the presence of a less intense positive CE partially masked by the tail of the stronger CE at 275 nm can be assumed (Fig. 3). Upon raising the [LPC]/[HSA] ratio, the magnitudes of the 275 and 298 nm CEs increased in a different manner: ICD values at 298 nm showed no further increase after reaching [LPC]/[HSA] ratio of 1, while the amplitude of the positive CE continued to rise (Fig. 8). This irregular behavior and the binding parameters estimated from ICD data suggest multiple, heterogeneous HSA binding of LPC. The term "heterogeneous binding" is used here in a CD spectroscopic sense meaning that

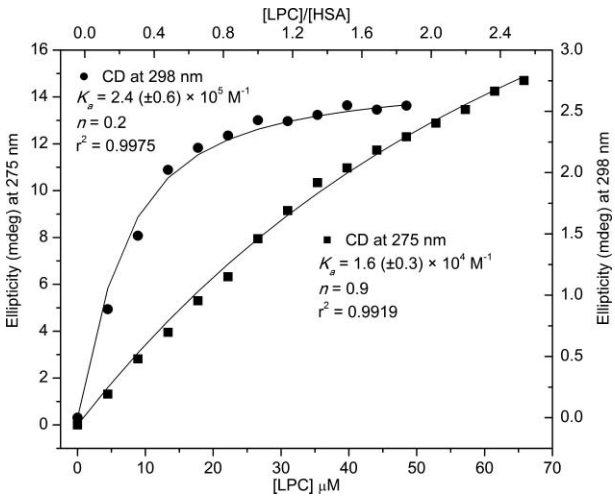

Fig. 8 Calculation of HSA binding parameters of LPC from ICD data measured in pH 7.4 Ringer buffer at 37 °C. ICD values recorded at 275 (left axis) and 298 nm (right axis) are plotted *vs.* molar concentrations of LPC ([HSA] = 25 μM). *Squares and circles*: experimental CD data points. *Solid lines*: results of curve fitting procedures. At the end of the titration the EtOH content of the sample was 2 v/v%.

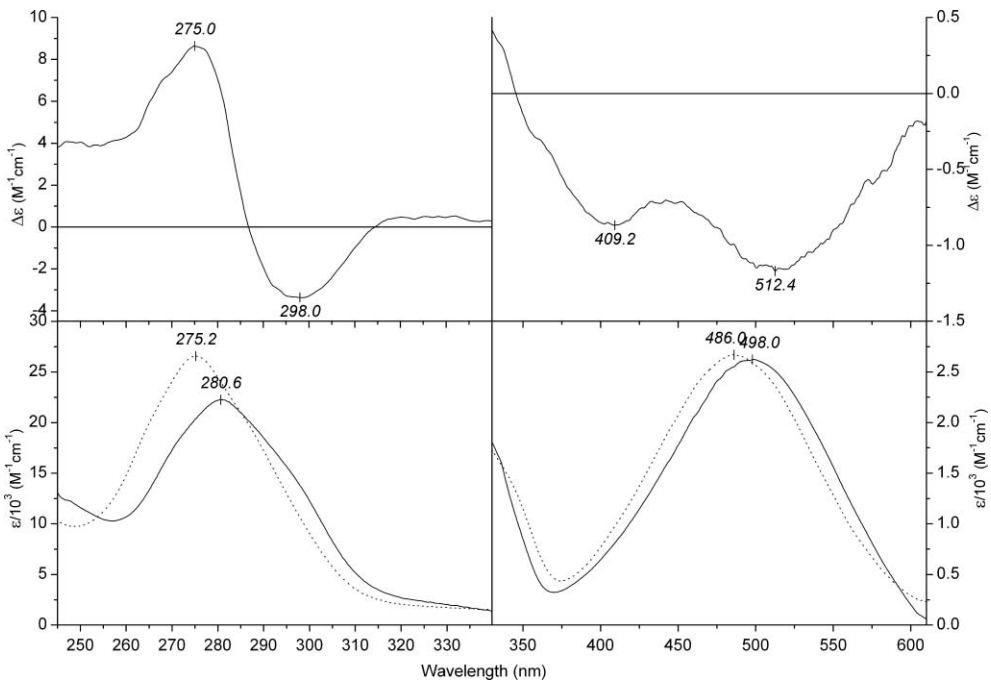

Fig. 7 Difference CD and UV/VIS absorption spectra of LPC in HSA solution at 37 °C. Left panels: [LPC] = 22 μM, [HSA] 25 μM. Right panels: [LPC] = 76 μM, [HSA] = 100 μM. Dotted lines: absorption spectrum of LPC in protein-free Ringer buffer solution (37 °C). Molar CD (Δε) and absorption (ε) values were calculated on the basis of total drug concentration of the sample solutions.

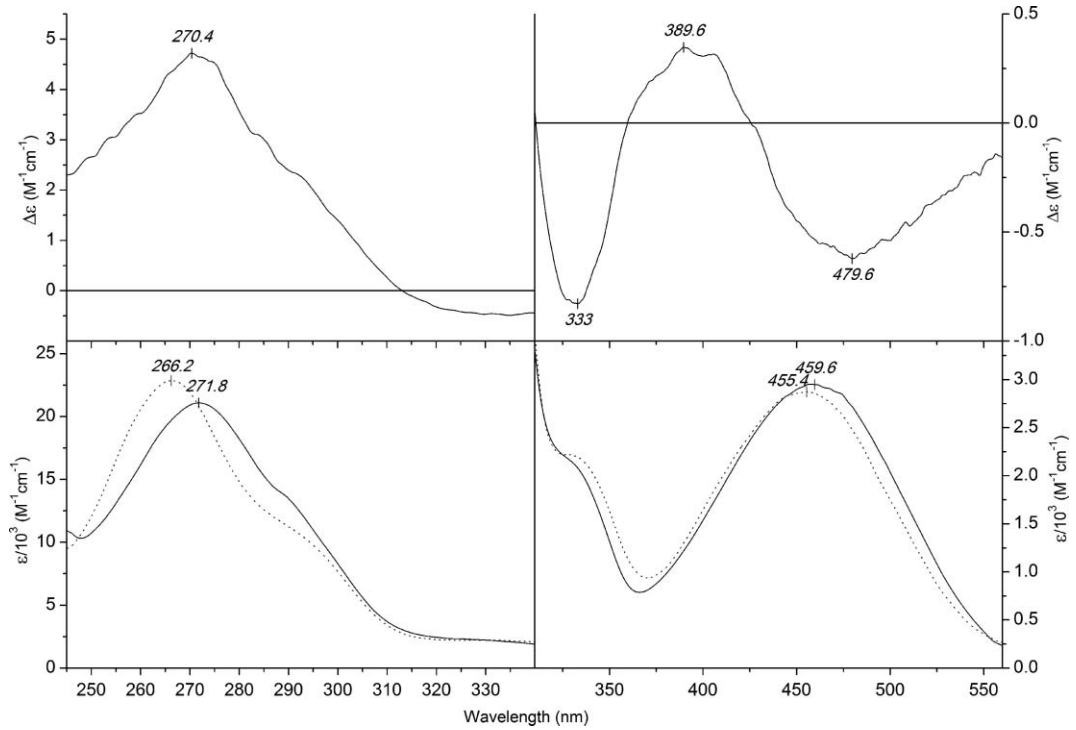

Fig. 9 Difference CD and UV/VIS absorption spectra of LWS in HSA solution at 37 °C. Left panels: [LWS] = 32 μM, [HSA] 40 μM. Right panels: [LWS] = 164 μM, [HSA] = 200 μM. Dotted lines: absorption spectrum of LWS in protein-free Ringer buffer solution (37 °C). Molar CD ($\Delta\varepsilon$) and absorption (ε) values were calculated on the basis of total drug concentration of the sample solutions. The EtOH content of the sample solutions was ≤2 v/v%.

the binding sites induce CD signals different in sign, intensity and spectral position. The calculated parameters are thus not reliable, since the formula used is valid only for a "homogeneous" binding process when spectroscopic profiles of CD bands induced by different binding sites are similar.[7]

CD-UV/VIS spectroscopy of LWS–HSA complexes

LWS is a natural dye ingredient of Henna produced in the leaves of the North African shrub *Lawsonia inermis*. LWS lacks any substituent in the C3 position and it is soluble in water. In buffer solution LWS exhibits a strong UV peak at 266 nm with a shoulder at about 290 nm and two additional medium intensity bands around 336 and 455 nm (Fig. 9). Distinctly from ATQ and LPC, the aqueous solution of LWS was yellow independent of the presence or absence of HSA, which is related to the higher excitation energy of its VIS absorption band (VIS λ_{max} of LWS is at shorter wavelengths by 35 nm). Besides the small bathochromic shifts of the UV and VIS absorption peaks, HSA binding of LWS induced four separated CEs between 245–560 nm (Fig. 9). CEs of LWS are weaker than those of ATQ but the shortest and longest-wavelength CEs are similar in sign and shape (*cf*. Fig. 3). Between 360 and 430 nm signs of the ICD bands of LWS and ATQ are opposite. The small negative CD shoulder of ATQ around 349 nm may be analogous to the negative CE of LWS at 333 nm. Due to the relatively weak ICD activity of LWS it was necessary to use high HSA and ligand concentrations for the CD titration experiment. Therefore, the CD titration of 200 μM HSA with 33–580 μM LWS was performed to determine the stoichiometry and the affinity of the binding. Analysis of the ICD values at 333 nm yielded 1.7×10^4 M^{-1} for K_a and 1.1 for n, respectively. Due to the poor signal/noise ratio ($\Delta\varepsilon/\varepsilon$), the 270 nm CE could do not be used to estimate the binding parameters.

CD-UV/VIS spectroscopic investigation of the interaction of ATQ, LPC and LWS with AAG

Since α_1-acid glycoprotein is another important drug carrier of human plasma,[20] ATQ–AAG interaction was also investigated by using CD and absorption spectroscopic methods under the same experimental conditions as applied for HSA studies. Artefacts in the CD spectrum of ATQ (data not shown) added to 27 μM AAG as well as the visible opalescence of the sample solution were indicative of the aqueous aggregation of the unbound drug molecules. Neither UV/VIS nor CD spectra of LPC and LWS were modified by the presence of AAG in relation to the spectra measured in AAG-free buffer solution (data not shown).

Displacement of fluorescent labels

5-Dimethylaminonaphthalene-1-sulfonamide (DMAS) and dansylsarcosine (DNSS) are the classical fluorescent labels of the two main HSA binding sites, called site I and site II, respectively.[21] The large site I was subdivided into three overlapping regions designated as Ia, Ib and Ic.[22] We investigated the effect of ATQ, LWS, LPC and some reference drugs for the binding of DNSS, DMAS and also of dansyl-L-asparagine (DNSA), which is a Ib specific probe. Fig. 10 shows the quenching effects for the three fluorescent probes. In the case of DNSS, ATQ and LPC provoked quenching effects similar to that of FLB ($K_{sv} = 3\ (\pm 0.5) \times 10^5$ M^{-1}),

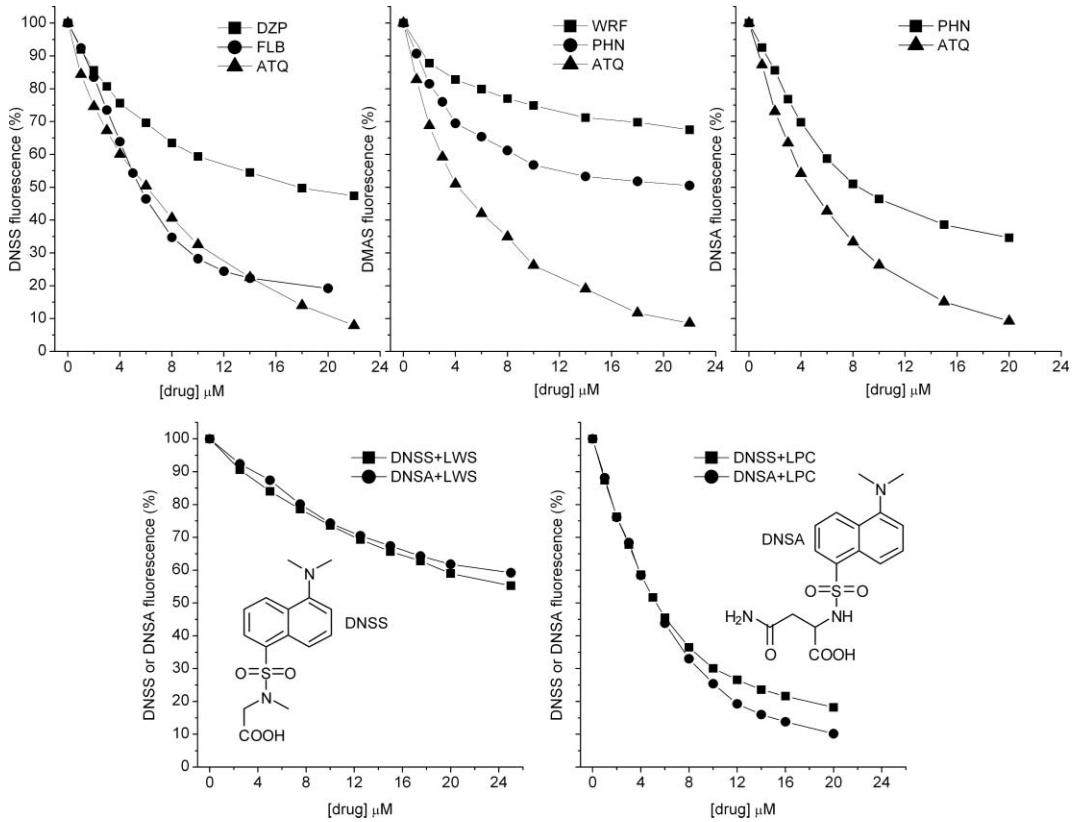

Fig. 10 Quenching effect of ATQ, LPC, LWS and HSA site marker drugs (DZP, FLB, PHN, WRF) on the fluorescence of specific probes (4 μM) in HSA solution (10 μM) at room temperature. λ_{exc}: 350 nm (370 nm for WRF), λ_{em}: 490 nm (480 nm for DNSS).

which is a high affinity ($K_a \approx 10^6$ M^{-1}) site II drug.[23,24] The quenching constant of LWS was about ten times smaller (3×10^4 M^{-1}), half that of DZP. In the case of the site I-specific DNSA and DMAS probes, ATQ also showed considerable displacement. Its quenching effects were about 3–4 times stronger (K_{sv} = 3.5 (±0.5) × 10^5 M^{-1}) compared to PHN, which is known to be a high affinity site I drug, located mainly at site Ib.[22] In the case of the DNSA label, the quenching effect of LPC was also similarly strong to that of ATQ, while LWS was about ten times weaker (3×10^4 M^{-1}). LPC and LWS were not measured with the DMAS label. These results suggest that ATQ and LPC have high, while LWS has low, affinities for both main binding sites of HSA. Since the high-affinity binding found for LPC could not be affirmed with the CD method (Fig. 8), the binding affinities were tested by an affinity chromatographic method too.

Binding test by affinity chromatography

The binding affinities of the ligands were evaluated from their retention on a short and low-capacity HSA-Sepharose column. Elution volumes ($V_e - V_{solvent}$) are characteristic of the binding affinity (ΣnK_a).[9] DZP was used as reference drug, with binding constant of about 1.8×10^5 M^{-1}.[17] ATQ could not be studied by this method because of its poor aqueous solubility. The results in Table 2 indicate that, compared to DZP, the binding of LWS is weaker, while LPC is about ten times stronger. The high-affinity binding of LPC is in accordance with the fluorescence displacement results.

Table 2 Elution volumes (V_e) obtained on a HSA-Sepharose column

Sample	V_e/mL
Solvent	3
DZP	14
LWS	10
LPC	≥120

Discussion

Binding of the achiral ATQ, LPC and LWS molecules to HSA induces multiple CEs both in the UV and VIS spectral regions and causes bathochromic shifts in the absorption bands (Fig. 3, 7 and 9). ICD data indicated that HSA can bind two ATQ molecules having similar CD contributions and high-affinity ($K_a \approx 10^6$ M^{-1}), one low-affinity ($K_a \approx 10^4$ M^{-1}) site for LWS, while a mixture of different CD contributions for LPC. Analysis of the ICD spectra provides information for the molecular details of the binding. The most intense CE measured at 275 nm coincides both in shape and spectral position with the strong UV band of ATQ associated to benzenoid and quinoid electron-transfer (E.T.) transitions of the hydroxynaphthoquinone nucleus.[25] CEs at higher wavelengths fall into the absorption regions of additional, medium intensity benzenoid/quinoid E.T. bands as well as the weak, totally masked $n \rightarrow \pi^*$ transitions of the quinone carbonyls above 400 nm. Accordingly, the longest wavelength CE can be ascribed to the chirally perturbed broad, quinoid E.T. band of ATQ centered about 500 nm. Since no separate absorption peak

can be seen in the spectral region of the negative CE at 406 nm this band probably is $n\rightarrow\pi^*$ by origin. It is reasonable to assume that the rigid naphthoquinone moiety preserves its planarity at the HSA binding sites, too. In that case, the $n\rightarrow\pi^*$ CD activity is induced by a nearby group placed asymmetrically in relation to the carbonyl moiety. For ATQ and LPC, the spatial orientation of the C3 substituent directed by the protein matrix will be decisive in determining the sign of the $n\rightarrow\pi^*$ CEs, which are negative for both drugs (Fig. 3 and 7). This suggests that in the HSA-bound state the C3 side-chain of ATQ and LPC is oriented in the same region of space around the ketone chromophores. For LWS, which lacks a C3 substituent, the $n\rightarrow\pi^*$ transitions can be perturbed by adjacent amino acid residues of the binding site which might give unequal, opposite contributions due to their different spatial orientations, and thus result in a weaker, positive $n\rightarrow\pi^*$ CE (Fig. 9). The couplet-like character of the UV CEs of LPC (Fig. 7) can be reminiscent of an intermolecular exciton coupling,[26] *i.e.* dipole–dipole coupling of π–π^* transitions of two LPC molecules bound close to each other. In that case, however, intensities of both CEs should reach saturation at the same [LPC]/[HSA] ratio and the value of n should be 2. Obviously, this is not the case (Fig. 8) so the exciton mechanism can be excluded. The opposite ICD bands of LPC at 275 and 298 nm can be ascribed to the heterogeneity of binding in a sense that distinct LPC binding sites can induce CD bands different in sign and intensity but close in energy. Superposition of such distinct ICD contributions precludes the calculation of real protein binding parameters, since we used a formula[7] which is valid only for a homogeneous binding process. Thus, the K_a value obtained from ICD titration data underestimates the HSA binding affinity of LPC (Fig. 8). Affinity chromatographic results (Table 2) indicated that its overall binding affinity ($K_a \approx 2 \times 10^6$ M^{-1}) is as high as that derived for ATQ. The similar ability of LPC to quench the fluorescence of site I and II markers DNSA and DNSS (Fig. 10) gives additional support for HSA binding properties similar to those of ATQ.

According to the spectroscopic results presented above, the high serum protein binding as well as the long plasma half-life of ATQ can be ascribed to its strong association with HSA at two binding sites (Fig. 4). Of note, strong HSA binding of several hydroxynaphthoquinone antimalarial agents have been reported[27] as early as in 1948. A very similar n value (2.56) was estimated for the HSA binding stoichiometry of the antimalarial 2-hydroxy-3-(2-methyloctyl)-1,4-naphthoquinone (coded as M-285 or SN-5949) suggesting analogous albumin binding behavior to that we found for ATQ.[28]

In order to identify the binding sites of ATQ on HSA the results obtained by various interaction experiments are to be considered. The effect of drugs on the ICD of ATQ indicated a rather complex behaviour. Binding competition observed by CD spectroscopy between FLB–ATQ (Fig. 6) refers to the accommodation of ATQ at drug site II, in subdomain IIIA of HSA. Data obtained with the drug site I marker IND, PHN and WRF, however, showed no unambiguous competitive displacement effect (Fig. 5). According to X-ray crystallographic studies, drug site I is more voluminous than site II[11,18] so compounds bound here do not fill the pocket entirely, allowing simultaneous accommodation of two ligand molecules.[7] Additional X-ray crystallographic results demonstrated the simultaneous binding of 3′-azido-3′-deoxythymidine and salicylate to site I and it has been proposed that this site is composed of three sub-sites which bind salicylate, IND and 3′-azido-3′-deoxythymidine, respectively.[29] Based on fluorescence spectroscopic studies performed with various site I ligands this area has also been divided into three, partly overlapping sub-sites designated as Ia, Ib, and Ic binding regions which can be labelled by acenocoumarol, DNSA and *n*-butyl-*p*-aminobenzoate, respectively.[22] As our fluorescence displacement experiments showed that ATQ effectively quenched the fluorescence of sub-site Ib marker DNSA, the binding of an ATQ molecule can be located in this region. On the other hand, in agreement with CD displacement results with FLB (Fig. 6), the quenching of fluorescence of the drug site II marker DNSS by ATQ corroborated its binding in subdomain IIIA, too. The weak displacement effect of DZP found in CD competition experiments (Fig. 6) and *vice versa*, the weak displacement of radioactive DZP by ATQ (Table 1) suggest the co-binding of DZP and ATQ at drug site II. It seems that the drug binding cavity in subdomain IIIA is also large and flexible enough to accommodate one ATQ and one DZP molecule simultaneously. This conclusion is in accordance with previous crystallographic results showing the adaptability of drug site II by co-binding of two molecules of long-chain fatty acids.[30,31] Taken together, ATQ binds to both principal drug sites of HSA where it leaves enough room for accommodation of other ligand molecules. However, there is no co-binding with bulky dansyl labels (Fig. 10). The entry of IND, WRF or PHN into the site I pocket might re-orientate the ATQ molecule bound there in relation to its asymmetric protein environment and/or might enable through-space chiral interactions between electronic transitions of the closely packed ligand chromophores.[26] It is likely that one or both of these mechanisms is responsible for modification of the ICD curves of ATQ observed during CD displacement experiments (Fig. 5).

Comparison of absorption spectra measured in alkaline EtOH and in protein-free pH 7.4 Ringer buffer shows the dominance of the dissociated, anionic form of ATQ in an aqueous environment (Fig. 2). It is reasonable since 2-hydroxy-1,4-naphthoquinone and its C3-substituted derivatives are acids, comparable in strength to R–COOH carboxylic acids, where 'R' group denotes the C3 substituents.[32,33] Although the pK_a of ATQ is not available, taking into consideration the pK_a values of related hydroxynaphthoquinones (LWS: 3.98,[33] LPC: 5.02,[34] phthiocol in which C3 is a methyl group: 5.08[35]), the majority of ATQ molecules should be dissociated at physiological pH. It seems, however, that the negative charge delocalized over the 2- and 4-oxygen atoms (Fig. 2) is unable to compensate the overall hydrophobicity of the molecule and thus enables only very low aqueous solubility.[10] In relation to ATQ, the water solubility of LPC, which bears a less bulky apolar C3 substituent, is so high that it can even be used as an acid–base indicator.[36] Accordingly, the pink coloration associated with the anionic form of ATQ cannot be observed in HSA-free buffer solution because of the very low concentration of the truly solvated species (Fig. 2). The presence of HSA, however, prevents the aggregation of ATQ by accommodating the ionized molecules at its binding sites. Therefore, it is questionable to use the neutral form for modeling ATQ–protein binding interactions. Computational docking of a non-dissociated ATQ molecule into the ubiquinol oxidation pocket of the yeast cytochrome bc_1 complex resulted in the formation of an intermolecular H-bond between the un-ionized hydroxyl group of ATQ and the imidazole

nitrogen of His181.[37–41] Being in an ionized state, the hydroxyl group cannot act as an H-donor but rather as an H-acceptor to the protonated nitrogen of the imidazole ring, as demonstrated in the case of the alkyl-6-hydroxy-4,7-dioxobenzothiazole which also binds to the yeast cytochrome bc_1 complex in anionic form.[42] Similarly to ATQ, the dissociation of the acidic hydroxyl group attached to the quinone moiety (pK_a is 6.5) appears in a color change of this compound from yellow to rose-violet.[42,43]

The marked difference in the color of LWS (yellow) and ATQ/LPC (pink) aqueous solutions can be rationalized by the positive inductive effect of the C3 substituent in the latter compounds which decreases the excitation energy of the quinoid E.T. band and shifts bathochromically the λ_{max} value close to 500 nm.

While ATQ and LPC bind avidly to HSA, the binding of LWS is about ten times weaker (Table 2) suggesting the important contribution of hydrophobic cyclohexyl-chlorophenyl or alkyl substituents to the binding. Hydrophobic interactions were also found to be decisive in determining the inhibitory potency of ATQ and related substances on different protein targets.[2,38–40,44] Fluorescence quenching results showed the contribution of both drug sites I and II in LWS binding to HSA (Fig. 10), but analysis of the ICD data at 333 nm indicated only one binding site. It suggests that binding to only one of the binding sites induces CD activity, while an LWS molecule accommodated at the other site remains 'CD silent' giving no contribution to the spectrum as seen in the case of binding of quinacrine to the F1/S genetic variant of AAG.[6] In the case of LWS there is no defined spatial orientation of the naphthoquinone moiety in relation to the asymmetric protein environment which is the prerequisite to obtain ICD signals. In a large binding cavity having several sub-sites like site I of HSA, the LWS molecule can adopt various orientations, the different ICD contributions of which cancel each other.

Comparison of HSA and AAG binding properties of ATQ indicates that AAG has no significant contribution in plasma protein binding of ATQ. Taking into consideration that basic antimalarial drugs bind principally to AAG,[6] it is unlikely that co-administration of these agents with ATQ would result in clinically relevant plasma protein drug–drug binding interactions.

Conclusions

In this study, by using CD-UV/VIS spectroscopy, fluorescent and radioactive marker displacements and affinity chromatographic methods, the characterization of HSA conjugates of ATQ, LPC and LWS has been achieved. HSA binding of these compounds induces polyphasic CEs allied to the UV/VIS electronic transitions of the naphthoquinone ring. CD and fluorescence displacement experiments showed that both drug binding sites I and II of HSA are involved in high- (ATQ, LPC) and low-affinity (LWS) binding of the substances. ICD spectra indicate that the binding topography in both sites are very similar for ATQ, while these are different for LPC. In the case of LWS binding only one site induced CD activity. Binding interaction results also suggested the possibility of co-binding of ATQ and some other drugs not only in the large drug site I pocket (PHN, WRF) but in site II (DZP), too. The weak HSA binding affinity obtained for LWS bearing no substituent in the C3 position suggests the importance of hydrophobic interactions established between the lipophilic C3 side-chain of ATQ/LPC and neighbouring protein residues. It can be predicted that albumin is the principal plasma binding protein for other natural (*e.g.* norlapachol, lomatiol) as well as synthetic (*e.g.* parvaquone, buparvaquone) 2-hydroxy-1,4-naphthoquinone compounds bearing bulky, apolar C3 substituents. Since the 2-hydroxy group of naphthoquinones dissociates at physiological pH, the anionic form should be taken into consideration in binding to other macromolecular targets, too.

Abbreviations

AAG	α_1-acid glycoprotein
ATQ	atovaquone
CD	circular dichroism
CE	Cotton effect
DMAS	5-dimethylaminonaphthalene-1-sulfonamide
DNSA	dansyl-L-asparagine
DNSS	dansylsarcosine
DZP	diazepam
E.T.	electron-transfer
FLB	flurbiprofen
HSA	human serum albumin
ICD	induced circular dichroism
IND	indomethacin
LPC	lapachol
LWS	lawsone
PHN	phenylbutazone
UV/VIS	ultraviolet-visible
WRF	warfarin

Acknowledgements

We thank GlaxoSmithKline for the supply of atovaquone. This work was supported by the research grant of OTKA K69213. Skilful technical assistance by Ilona Kawka is appreciated.

References

1 M. Schlitzer, *ChemMedChem*, 2007, **2**, 944.
2 J. J. Kessl, S. R. Meshnick and B. L. Trumpower, *Trends Parasitol.*, 2007, **23**, 494.
3 P. E. Rolan, A. J. Mercer, E. Tate, I. Benjamin and J. Posner, *Antimicrob. Agents Chemother.*, 1997, **41**, 1319.
4 G. A. Butcher and R. E. Sinden, *Am. J. Trop. Med. Hyg.*, 2003, **68**, 111.
5 J. L. Miller and L. A. Trepanier, *Eur. J. Clin. Pharmacol.*, 2002, **58**, 69.
6 F. Zsila, J. Visy, G. Mády and I. Fitos, *Bioorg. Med. Chem.*, 2008, **16**, 3759.
7 F. Zsila, Z. Bikadi and M. Simonyi, *Biochem. Pharmacol.*, 2003, **65**, 447.
8 J. R. Lakowicz, *Principles of Fluorescence Spectroscopy*, Springer Science+Business Media, LLC: New York, 3rd edn, 2006.
9 I. Fitos, Z. Tegyey, M. Simonyi, I. Sjöholm, T. Larsson and C. Lagercrantz, *Biochem. Pharmacol.*, 1986, **35**, 263.
10 E. Nicolaides, E. Galia, C. Efthymiopoulos, J. B. Dressman and C. Reppas, *Pharm. Res.*, 1999, **16**, 1876.
11 S. Curry, *Drug Metab. Pharmacokinet.*, 2009, **24**, 342.
12 G. A. Ascoli, E. Domenici and C. Bertucci, *Chirality*, 2006, **18**, 667.
13 B. Ekman, T. Sjödin and I. Sjöholm, *Biochem. Pharmacol.*, 1980, **29**, 1759.
14 J. H. Perrin and D. A. Nelson, *Life Sci.*, 1972, **11**, 277.
15 S. Watanabe and T. Saito, *Biochem. Pharmacol.*, 1992, **43**, 931.
16 I. Fitos, J. Visy, F. Zsila, G. Mády and M. Simonyi, *Bioorg. Med. Chem.*, 2007, **15**, 4857.
17 I. Sjöholm, B. Ekman, A. Kober, I. Ljungstedt-Pahlman, B. Seiving and T. Sjödin, *Mol. Pharmacol.*, 1979, **16**, 767.

18 J. Ghuman, P. A. Zunszain, I. Petitpas, A. A. Bhattacharya, M. Otagiri and S. Curry, *J. Mol. Biol.*, 2005, **353**, 38.
19 H. Hussain, K. Krohn, V. U. Ahmad, G. A. Miana and I. R. Green, *Arkivoc*, 2007, 145.
20 Z. H. Israili and P. G. Dayton, *Drug Metab. Rev.*, 2001, **33**, 161.
21 G. Sudlow, D. J. Birkett and D. N. Wade, *Mol. Pharmacol.*, 1975, **11**, 824.
22 K. Yamasaki, T. Maruyama, U. Kragh-Hansen and M. Otagiri, *Biochim. Biophys. Acta, Protein Struct. Mol. Enzymol.*, 1996, **1295**, 147.
23 B. Honoré and R. Brodersen, *Mol. Pharmacol.*, 1984, **25**, 137.
24 S. Wanwimolruk, D. J. Birkett and P. M. Brooks, *Mol. Pharmacol.*, 1983, **24**, 458.
25 I. Singh, R. T. Ogata, R. E. Moore, C. W. J. Chang and P. J. Scheuer, *Tetrahedron*, 1968, **24**, 6053.
26 F. Zsila, Z. Bikádi and M. Simonyi, *Tetrahedron: Asymmetry*, 2001, **12**, 3125.
27 H. Heymann and L. F. Fieser, *J. Pharmacol. Exp. Ther.*, 1948, **94**, 97.
28 A. E. Reif, *Arch. Biochem. Biophys.*, 1953, **47**, 396.
29 L. Zhu, F. Yang, L. Chen, E. J. Meehan and M. Huang, *J. Struct. Biol.*, 2008, **162**, 40.
30 J. R. Simard, P. A. Zunszain, J. A. Hamilton and S. Curry, *J. Mol. Biol.*, 2006, **361**, 336.
31 A. A. Bhattacharya, T. Grune and S. Curry, *J. Mol. Biol.*, 2000, **303**, 721.
32 M. G. Ettlinger, *J. Am. Chem. Soc.*, 1950, **72**, 3085.
33 L. F. Fieser, E. Berliner, F. J. Bondhus, F. C. Chang, W. G. Dauben, M. G. Ettlinger, G. Fawaz, M. Fields, M. Fieser, C. Heidelberger, H. Heymann, A. M. Seligman, W. R. Vaughan, A. G. Wilson, E. Wilson, M. I. Wu, M. T. Leffler, K. E. Hamlin, R. J. Hathaway, E. J. Matson, E. E. Moore, M. B. Moore, R. T. Rapala and H. E. Zaugg, *J. Am. Chem. Soc.*, 1948, **70**, 3151.
34 E. G. Ball, *J. Biol. Chem.*, 1936, **114**, 649.
35 E. G. Ball, *J. Biol. Chem.*, 1934, **106**, 515.
36 K. C. Joshi, P. Singh and G. Singh, *Talanta*, 1976, **23**, 325.
37 J. J. Kessl, B. B. Lange, T. Merbitz-Zahradnik, K. Zwicker, P. Hill, B. Meunier, H. Palsdottir, C. Hunte, S. Meshnick and B. L. Trumpower, *J. Biol. Chem.*, 2003, **278**, 31312.
38 J. J. Kessl, P. Hill, B. B. Lange, S. R. Meshnick, B. Meunier and B. L. Trumpower, *J. Biol. Chem.*, 2004, **279**, 2817.
39 J. J. Kessl, N. V. Moskalev, G. W. Gribble, M. Nasr, S. R. Meshnick and B. L. Trumpower, *Biochim. Biophys. Acta, Bioenerg.*, 2007, **1767**, 319.
40 J. J. Kessl, K. H. Ha, A. K. Merritt, B. B. Lange, P. Hill, B. Meunier, S. R. Meshnick and B. L. Trumpower, *J. Biol. Chem.*, 2005, **280**, 17142.
41 L. M. Hughes, R. Covian, G. W. Gribble and B. L. Trumpower, *Biochim. Biophys. Acta, Bioenerg.*, 2010, **1797**, 38.
42 H. Palsdottir, C. G. Lojero, B. L. Trumpower and C. Hunte, *J. Biol. Chem.*, 2003, **278**, 31303.
43 B. L. Trumpower and J. G. Haggerty, *J. Bioenerg. Biomembr.*, 1980, **12**, 151.
44 M. Hansen, J. Le Nours, E. Johansson, T. Antal, A. Ullrich, M. Loffler and S. Larsen, *Protein Sci.*, 2004, **13**, 1031.

